

2-Grating Inelastic Free Electron Interferometry

Cameron Johnson¹, Amy Turner², F. Javier Garcia de Abajo³ and Benjamin McMorrان²

¹University of Oregon, EUGENE, Oregon, United States, ²University of Oregon, United States, ³ICFO-Institut de Ciències Fòtoniques, Castelldefels, Catalonia, Spain

We construct a scanning 2-grating Mach-Zehnder interferometer (2GMZI) for free electrons in a transmission electron microscope (TEM). With the 2GMZI we measure the spectrally resolved interference of free electrons inelastically scattered from a localized plasmon resonance (LPR) of a single metallic nanoparticle (NP).

Interferometric studies of inelastically scattered free electrons in a TEM have been used to study coherence properties and entanglement with a specimen [1, 2, 3]. These typically involve electron holography, dividing and shearing the wavefront with an electrostatic biprism for self interference, requiring a high degree of spatial coherence [4]. Amplitude division with nanoscale gratings [5, 6] as beamsplitters mitigates this requirement as overlapping the spatially separated paths forms an image of the input grating with a one to one spatial alignment of the two paths [7]. Inserting a second grating with the same pitch and orientation of the image of the input grating superimposes and recombines the two spatially separated paths to be co-propagating, forming a 2GMZI.

The scanning 2GMZI is constructed by placing SiN phase gratings in the condenser 2 and selected area aperture planes of an image-corrected FEI Titan TEM operated at 80 keV. The gratings are optimized to create 2 probes at the specimen plane [8], which are then recombined in the interferometer output and collected by the entrance aperture of an EELS spectrometer (Fig. 1). The relative phase between the two probes in the output is due to the interactions with the sample, as well as the relative lateral alignment of the input and output gratings, $\Delta\phi(\mathbf{r}) = \Delta\phi^{\{\text{sample}\}}(\mathbf{r}) + \Delta\phi^{\{\text{align}\}}$. The alignment phase can be held constant, independent of the geometric scan/descan shifts applied to raster the probes across the specimen. Thus the intensity of the interferometer output oscillates solely as a function of the external phases applied to the probes while the alignment phase can be separately controlled to shift the spatial interference fringes.

The LPR electron energy loss probability for 2 probes passing by a spherical metallic NP can be expressed as the sum of the 2 one-probe loss probabilities and an interference term. The dominant response is dipolar, and when each probe is on either side of the NP the EELS interference term is proportional to $\cos(\Delta\phi - \pi)$, whereas the interference term for the intensity of the bare interferometer is $\cos(\Delta\phi)$. This converse relation can be seen in the intensity of the zero loss peak (ZLP) and the dipole plasmon peak of the EELS spectrum (Fig. 2(a-c)).

With the 2GMZI set to have a probe separation of 70 nm, we demonstrate the interference of free electrons inelastically scattered from plasmonic excitations of a 30 nm radius spherical gold NP on a lacey carbon support (Fig. 2(d-f)). The spatially dependent interferometer output intensity is consistent with the theoretical predictions with a realistic external phase caused by the potential from static surface charge on the sample.

Further development of this free electron interferometric platform in a TEM shows promise for the coherent control of the free electron wavefunction [9], selective excitation of arbitrary plasmonic modes [10], exploration of decoherence theory [11, 12], and has the potential for including multimodal functionality such as cathodoluminescence [13].

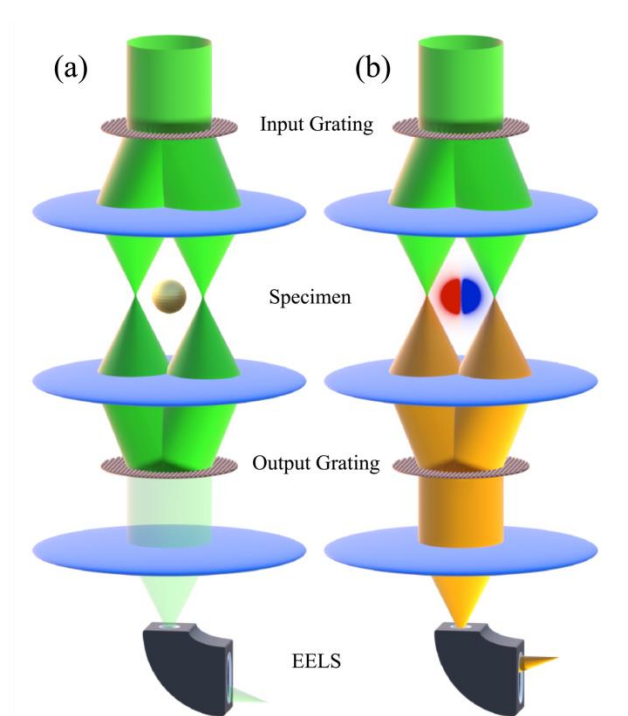


Figure 1. Illustration of 2GMZI elastic ZLP component; right, dipole plasmon scattered component resolved with an EELS spectrometer. Illustration of 2GMZI for the (a) elastic ZLP component, and the (b) dipole plasmon scattered component resolved with an EELS spectrometer.

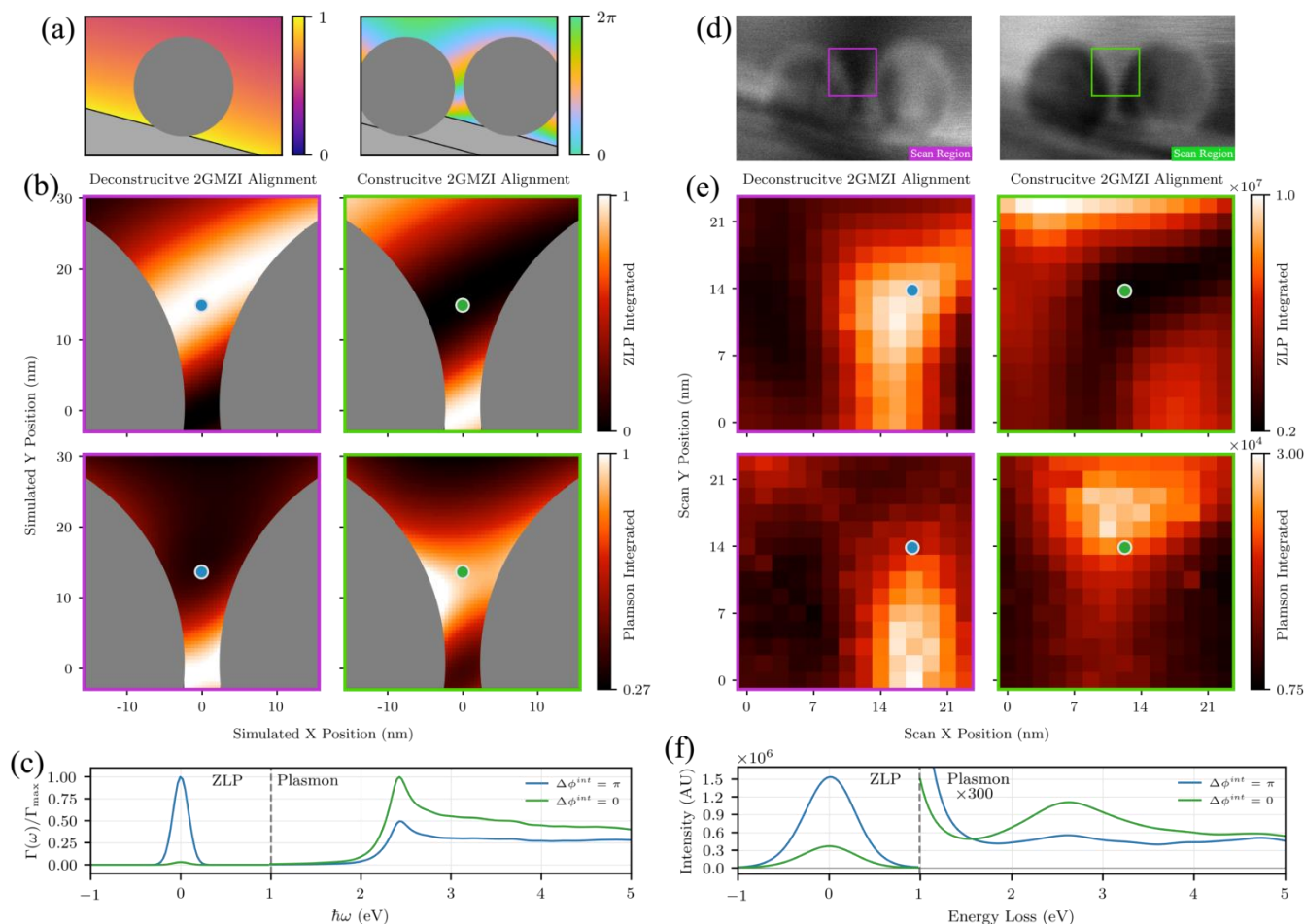


Figure 2. (a) Left, simulated static projected potential $V(x,y)=V_{\text{max}}$; right, 2-probe relative external phase due to simulated projected potential, $\Delta\phi\{\text{sample}\}$, for a metallic NP on a carbon support. (b) Simulated spatially varying interference for: top ZLP integrated, and bottom plasmon integrated spectrum images. Purple outlines correspond to deconstructive interferometer output, $\Delta\phi\{\text{align}\}=\pi$, and green outlines to constructive interferometer output, $\Delta\phi\{\text{align}\}=0$. (c) Simulated EELS spectra from location of colored spot corresponding to color of the plot line. (d) 2GMZI bright field images of 30 nm radius gold NP with deconstructive and constructive interferometer alignments showing spectrum image scan regions on the left and right respectively. (e,f) Experimental data with same conditions as simulated data in (b,c).

References

- [1] H Lichte and B. Freitag. Ultramicroscopy, 81(3):177-186, April 2000.
- [2] P. Schattschneider and H. Lichte. Phys. Rev. B, 71(4):045130, January 2005.
- [3] P. L. Potapov, et. al. Ultramicroscopy, 107(8):559-567, August 2007.
- [4] T. Latychevskaia. Ultramicroscopy, 175:121-129, April 2017.
- [5] B. J. McMorran, et. al. Ultramicroscopy, 106(4):356-364, March 2006.
- [6] T. R. Harvey, et. al. New J. Phys., 16(9):093039, September 2014.
- [7] F. S. Yasin, et. al. J. Phys. D: Appl. Phys., 51(20):205104, April 2018.
- [8] C. W. Johnson, et. al. Appl. Opt., 59(6):1594-1601, February 2020.
- [9] K. E. Echternkamp, et. al. Nature Phys, 12(11):1000-1004, November 2016.

- [10] G. Guzzinati, et. al. *Nat Commun*, 8(1):1-8, April 2017.
- [11] A. Howie. *Ultramicroscopy*, 111(7):761-767, June 2011.
- [12] N. Kerker, et. al. *New J. Phys.*, 22(6):063039, June 2020.
- [13] A. Polman, et. al. *Nat. Mater.*, 18(11):1158-1171, November 2019.